THE JOURNAL OF PHYSICAL CHEMISTRY B

Article

pubs.acs.org/JPCB

Picosecond Kinetics of Strongly Coupled Excitons and Surface Plasmon Polaritons

Daniel E. Gómez,*[,†,‡] Shun Shang Lo,[§] Timothy J. Davis,[‡,∥] and Gregory V. Hartland*[,§]

[†]School of Physics, The University of Melbourne, Parkville, Victoria 3010, Australia

[‡]Materials Science and Engineering, CSIRO, Clayton, Victoria 3169, Australia

[§]Department of Chemistry and Biochemistry, University of Notre Dame, Notre Dame, Indiana 46556-5670, United States

[∥]Melbourne Centre for Nanofabrication, 151 Wellington Road, Clayton, Victoria 3168, Australia

Supporting Information

ABSTRACT: Coupling between excitons of CdSe nanocrystal quantum dots (NQDs) and surface plasmon polaritons (SPPs) of an Ag film attached to a prism have been studied by steady-state and transient reflectivity measurements in the Kretschmann geometry. In these experiments, the angle of incidence of the probe beam selects hybrid exciton/SPP states with different wavevectors and exciton/SPP compositions. The dynamics measured in the transient reflectivity experiments are sensitive to the composition of the hybrid states. Specifically, fast dynamics are observed at probe wavevectors where the lower hybrid state has predominant SPP character. In contrast, at probe wavevectors where the lower hybrid state is predominantly excitonic, the dynamics are similar to that measured for CdSe NQDs on glass.

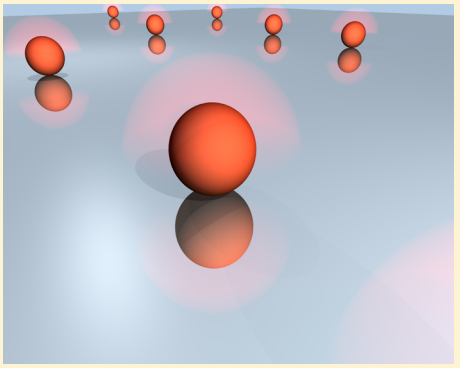

INTRODUCTION

A step forward in plasmonics, nanoscale optics with surface plasmon polaritons (SPPs),[1] is the realization of active control over SPP properties such as resonance frequencies and propagation lengths. This type of control can be achieved through the integration of the (passive) plasmonic supporting nanostructures with materials exhibiting optical properties that can change with the application of external stimuli such as changes in temperature,[2] mechanical stress,[3] electrical currents or voltages,[4−7] chemical changes,[8−11] and optical signals.[12−17] The development of active plasmonics has important technological implications; for example, it could lead to devices that incorporate both electronic and optical functionalities at the nanoscale.[18]

Nanocrystal quantum dots (NQDs)[19] are a class of materials that exhibit size-tunable optical properties, are very photostable, and possess high photoluminescence quantum yields, making them attractive candidates for developing active plasmonic devices. These materials have been used in conjunction with plasmonic structures where the strong electromagnetic fields associated with SPPs have been employed to enhance the fluorescence of NQDs[20−23] and the rates of energy transfer among NQDs.[24] NQDs have also been used for the generation of single plasmons[25] and for controlling the plasmon propagation in planar structures.[26] These applications rely on the interaction between the electromagnetic fields produced by the surface plasmons (collective oscillations of electrons at metal−dielectric interfaces) and the electronic excitations in the nanocrystals: excitons. In most of these examples, these interactions take place in the weak-coupling regime where the wave functions of the electronic excitations are only slightly perturbed. In the strong coupling regime, the optical properties of the interacting system are described in terms of hybrid plasmon−exciton states, where the wave functions of the initial excitonic and surface plasmon states are strongly mixed. This interaction regime has been experimentally achieved with *J* aggregates of organic molecules,[27−34] organic dye molecules in thin films,[35] and organic−inorganic Perovskites[32] as well as with CdSe NQDs.[36−38]

Here, we present an experimental study on the strong interaction of electronic excitations in nanocrystal quantum dots with SPPs supported on the simplest plasmonic structure: a thin nanometer scale metal film. By means of transient pump−probe spectroscopy, we studied the dynamical aspects of this interaction. These measurements demonstrate that the rate of energy relaxation in the mixed exciton−SPP states can be an order of magnitude faster than that for a pure CdSe film.

SAMPLE PREPARATION AND STEADY-STATE MEASUREMENTS

The CdSe nanocrystal samples were synthesized following the method of van Embden and Mulvaney.[39] In order to achieve

Special Issue: Paul F. Barbara Memorial Issue

Received: July 10, 2012
Revised: September 28, 2012
Published: October 1, 2012

   dx.doi.org/10.1021/jp306830s | *J. Phys. Chem. B* 2013, 117, 4340−4346

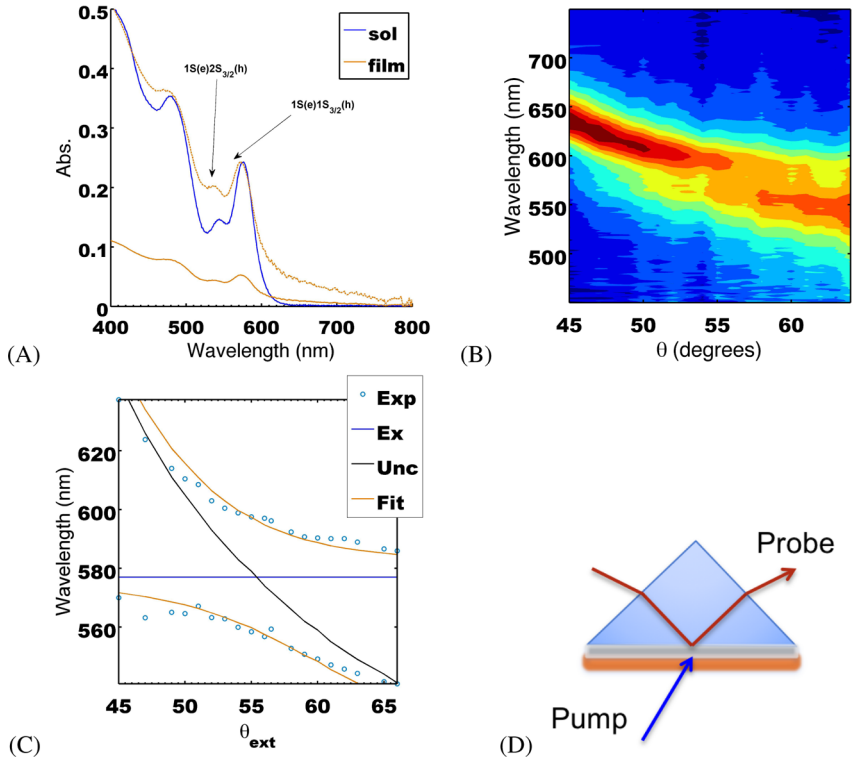

Figure 1. (A) Absorption spectra of the CdSe QDs in solution (sol) and in the thin film on glass (film). The latter is also shown normalized to match the absorption of the first exciton transition observed in solution. (B) Steady-state reflectivity spectra, presented as R_p/R_s, measured at the indicated angles of incidence. The spectra consist of two features with an avoided crossing that occurs at the position of the lowest-energy transition of the absorption spectra. (C) Wavelength vs angle diagram obtained from the reflectivity spectra, shown along with a coupled oscillator model[37] ("Fit") that gives a resonance splitting of ~136 meV. "Unc" is the dispersion curve expected from the uncoupled SPP; "Exp" are the experimental data points obtained from panel B; "Exc" is the exciton transition energy. (D) Diagram of the pump–probe experiment.

closely-packed and uniform films, the ligands that passivate the surface of the nanocrystals were exchanged with pyridine by overnight heating at 70 °C under a nitrogen atmosphere and constant stirring. The samples were subsequently washed by precipitation with *n*-hexane and centrifugation, redispersed in pyridine, and filtered with 0.2 μm filters resulting in the absorption spectrum (in solution) shown in Figure 1A. From the position of the first absorption feature on this plot, the mean diameter of the CdSe nanocrystals can be estimated to be approximately 3.9 nm.[40] Thin films were made by spin-coating small amounts of this nanocrystal dispersion onto clean substrates. On glass, the resulting films had an absorption spectrum shown in Figure 1A. The interaction between the SPPs of Ag and the CdSe excitons in the films was studied via angle-dependent, attenuated total reflection (ATR) reflectivity measurements. To this end, thermally evaporated Ag films (supported on glass) of 59 nm thickness were coated, by spin-coating, with CdSe NQDs to ~39 nm in thickness (see Supporting Information for AFM topography of the films). The thickness of the Ag films ensures the formation of continuous films and also allows for the excitation of SPPs at the Ag/air interface in the Kretschmann configuration.[41] In this arrangement, white light is incident at the base of a right angle glass (SF10) prism, onto which the Ag/CdSe coated coverslip was attached using an index matching oil. The steady-state spectra of the reflected p-polarized light were measured relative to that of the s-polarization with a fiber-coupled spectrometer (Ocean Optics, ADC1000-USB) using a white light source (Thorlabs, OSL-1). The results are shown in Figure 1B.

The reflectivity spectra in Figure 1B consist of two dips that change both in wavelength position (their minima) and relative intensities as the angle of incidence changes. Moreover, these spectral dips show an avoided crossing only at the position of the lowest-energy exciton transition of the CdSe NQDs, which is shown in Figure 1C. This avoided crossing or Rabi splitting has been interpreted as arising from strong exciton–plasmon coupling in these films,[36,37] which theoretically result from the formation of hybrid plasmon–exciton states. At the angle corresponding to the avoided crossing in Figure 1C, the wave functions are strongly mixed, and the system is best represented by hybrid states composed of equal plasmon and exciton contribution.

The static measurements in Figure 1C demonstrate that there is strong coupling between the plasmons in the silver film and the excitons of the CdSe quantum dots. The goal of this article is to investigate the dynamics of these coupled states. Specifically, to determine whether the degree of mixing (which can be controlled by the angle of incidence in our experiments) affects the energy relaxation of the different states and (conversely) to investigate how excitation of the CdSe quantum dots affects the mixing. To this end, we performed transient pump–probe measurements.

TRANSIENT PUMP–PROBE MEASUREMENTS

These experiments were conducted using a Clark-MXR 2010 laser system (775 nm, 1 mJ/pulse, fwhm = 130 fs, 1 kHz repetition rate), from which the pump pulses were generated with 95% of the fundamental and frequency doubled to 387 nm. The probe pulses were generated with the remaining 5% of

dx.doi.org/10.1021/jp306830s | J. Phys. Chem. B 2013, 117, 4340–4346

the fundamental focused on a sapphire plate to produce a white-light continuum. The pump pulses were directed onto the air/CdSe side of the Prism/Ag/CdSe system, exciting the CdSe film (see diagram in Figure 1D) and creating high energy electron−hole pairs in the NQDs, which relax on a picosecond time scale into the low-energy states.[19] The pump power at the sample was 2.8 mW (~0.06 W/cm^2), which is insufficient to generate multiple excitons. Probe pulses with p-polarization were directed to the prism/Ag/CdSe side of the films at variable angles of incidence. In this configuration, the probe monitors the hybrid plasmon−exciton states, much like in the steady-state experiments shown in Figure 1. However, the excitation of the CdSe film by the pump laser modifies the interaction between the SPPs and the excitons, leading to changes in the reflectivity spectrum that are related to both the energy relaxation of the CdSe excitons, and their coupling to the SPPs. The reflected probe beam was collected with a fiber-coupled CCD spectrograph (Ocean Optics, S2000 UV−vis) providing a 450−800 nm data window. Time-resolved pump-induced reflectivity changes were recorded by delaying the probe pulses relative to the pump pulses with a mechanical stage.[42]

As a reference point for our discussion, in Figure 2 (top), we show the transient differential reflectivity spectra, $\Delta R/R = (R_{pump} - R_{no\ pump})/R_{no\ pump}$ of a film of CdSe nanocrystals deposited on a glass substrate (that is, without SPP coupling). The spectra consist of a number of asymmetric dispersive lineshapes, at positions displaced from those of the steady-state absorption spectra of Figure 1A. The features in the transient reflectivity spectra derive from the frequency dependent dielectric permittivity of the CdSe layer $\varepsilon(\omega)$. To gain a qualitative understanding of the origin of these features and their line shape, we model this permittivity as a single Lorentzian $\varepsilon(\omega) = \varepsilon_b + f_0/(\omega_0^2 - \omega^2 - i\Gamma\omega)$, where ε_b is the background dielectric permittivity and f_0 is the oscillator strength of the electronic transition occurring at the frequency ω_0 (with an associated damping constant Γ). Fits to the steady-state reflectivity data of the CdSe films on glass (for which ω_0 = 2.149 eV) and on the Ag films, using the Fresnel equations, yield values of f_0 = 0.03, ε_b = 3.53, and $\hbar\Gamma$ = 0.1 eV (see Supporting Information, for details, and Figure 1C).

The effect of the pump in the transient measurements is to promote electrons/holes to high-energy states in the conduction/valence bands of the NQDs. For the CdSe NQDs on glass, these charge carriers rapidly relax to the band-edge producing a bleach due to state filling and spectral shifts of the exciton transition from the electric fields associated with trapped charge carriers.[43] Within the simple single Lorentzian model, the bleach decreases the oscillator strength of the exciton transition according to $f = f_0/(1 + n)$ where n is a parameter related to the exciton population created by the pump pulse.[16,44] This modifies the permittivity of the CdSe film and changes how the film reflects the time-delayed probe light. Figure 3A (top) shows an experimental $\Delta R/R$ spectra for the CdSe film on glass, recorded at 1 ps delay. A calculated spectrum is presented in Figure 3B (top) using the single Lorentzian model for $\varepsilon(\omega)$ in the Fresnel equations with n = 0.08 (details in the Supporting Information).

Although quantitatively incorrect, the calculated spectrum reproduces the form of the experimental spectrum. In particular, there is an increased reflectance ($\Delta R/R > 0$) to the red of the exciton transition that exceeds the decreased reflectance ($\Delta R/R < 0$) observed at higher frequencies. There

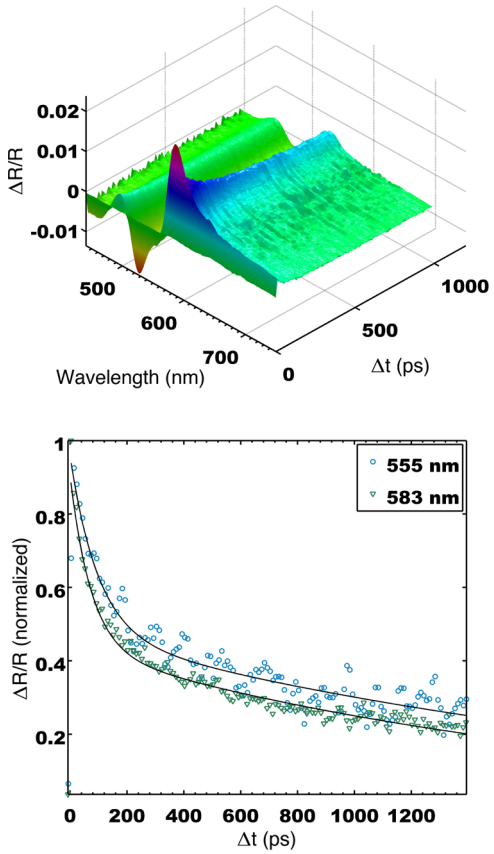

Figure 2. (top) Transient reflectivity spectra of a film of CdSe nanocrystals on a glass substrate, measured at the pump−probe delay times indicated in the figure. The data is shown as $\Delta R/R$: change in the reflectivity of the probe pulses induced by the nonresonant pump. The reflectivity of the p-polarized probe pulses was measured at 45° incidence. (bottom) Normalized kinetic traces ($\Delta R/R$ vs delay time) of the spectral features at 583 nm (triangles) and 555 nm (circles, multiplied by −1). The plot also includes biexponential fits (lines), as discussed in the text.

are several differences between the experimental and modeled $\Delta R/R$ spectra that arise from the fact that there are other electronic transitions occurring at higher frequencies in the CdSe film that also experience transient effects. These contributions appear as additional features on the blue side of the spectrum and would require additional Lorentzians in the model for $\varepsilon(\omega)$.

The single Lorentzian model described above gives a simple description of the dynamics observed for the CdSe film on glass. Bleaching of the lowest-energy exciton transition produces an asymmetric $\Delta R/R$ spectrum whose magnitude (value of $\Delta R/R$) is dictated by the amount of saturation experienced by the CdSe film (or n in the Lorentzian model). Decay of population out of the lowest exciton state then leads to a decrease in both the positive and negative $\Delta R/R$ features. In Figure 2 (bottom), we show the measured decay of these two $\Delta R/R$ spectral features (one was multiplied by −1 for clarity), and it can be clearly seen that, within experimental noise, the two decays are almost identical. The kinetics of this decay are highly nonexponential and can be fit to a biexponential function (the time constants are given in Table 1). The initial fast decay is attributed to electron trapping at defect states, and the slow decay is assigned to interband relaxation, by either radiative or nonradiative processes (at the

dx.doi.org/10.1021/jp306830s | J. Phys. Chem. B 2013, 117, 4340−4346

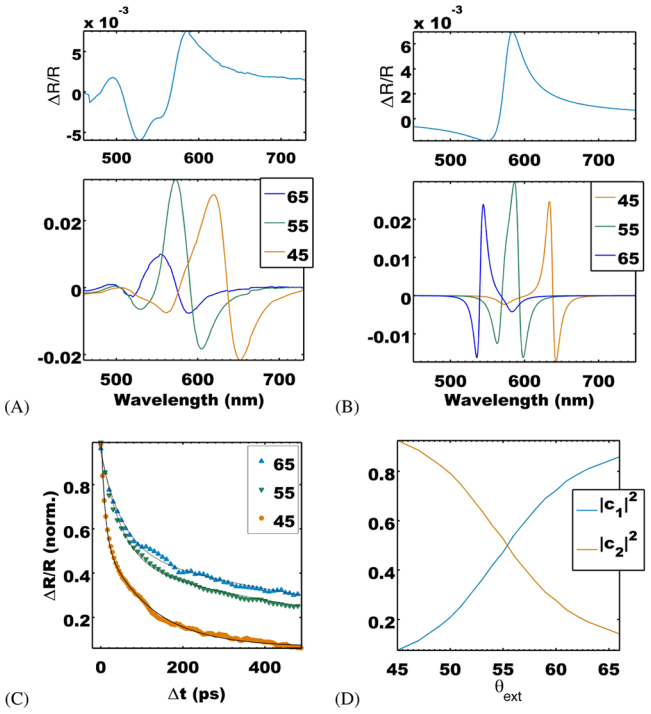

Figure 3. (A) $\Delta R/R$ spectra for (top) a film of CdSe QDs on glass and (bottom) CdSe films on Ag. (B) Predictions of a simple Lorentzian model for $\varepsilon(\omega)$ for a film of 39 nm in thickness, with $\sqrt{\varepsilon_b} = 1.88$, $\hbar\omega_0 = 577$ nm, $\hbar\Gamma \approx 0.1$ eV, $f = 0.03$, and $n = 0.08$ (see text for details). The plot in the top panel is for a bare film of the dielectric, whereas the plot in the bottom panel corresponds to a Ag/dielectric film. (C) Normalized decay traces of the $\Delta R/R$ data for the bands observed at 554, 572, and 614 nm at the angles indicated in the figure. (D) Plot of the absolute value of the mixing coefficients of the hybrid exciton–plasmon states vs angle for the lower polariton branch of Figure 1C.

low pump fluences used in our experiments, effects such as Auger recombination are negligible).[19,45−48]

To study the kinetics of energy relaxation in the strongly coupled SPP–exciton system, we directed the pump pulses to the CdSe side of the Ag/CdSe films mounted on a right-angle prism. The change in reflectivity of p-polarized white light pulses in the Kretschmann configuration induced by the pump laser was then monitored as a function of pump–probe delay. The reflectivity was measured at different angles of incidence for the probe beam: 45° [results shown in Figure 4A], 55° [shown in Figure 4B], and 65° [shown in Figure 4C]. These angles correspond to cases where the SPPs are tuned to the red and close to resonance with and to the blue of the lowest energy exciton transition, respectively [see Figure 1C]. The $\Delta R/R$ spectra recorded at 0.5 ps pump–probe delay are presented together in Figure 3A for comparison. All the measured $\Delta R/R$ spectra consist of two features of opposing sign at longer wavelengths followed by (at least one) negative

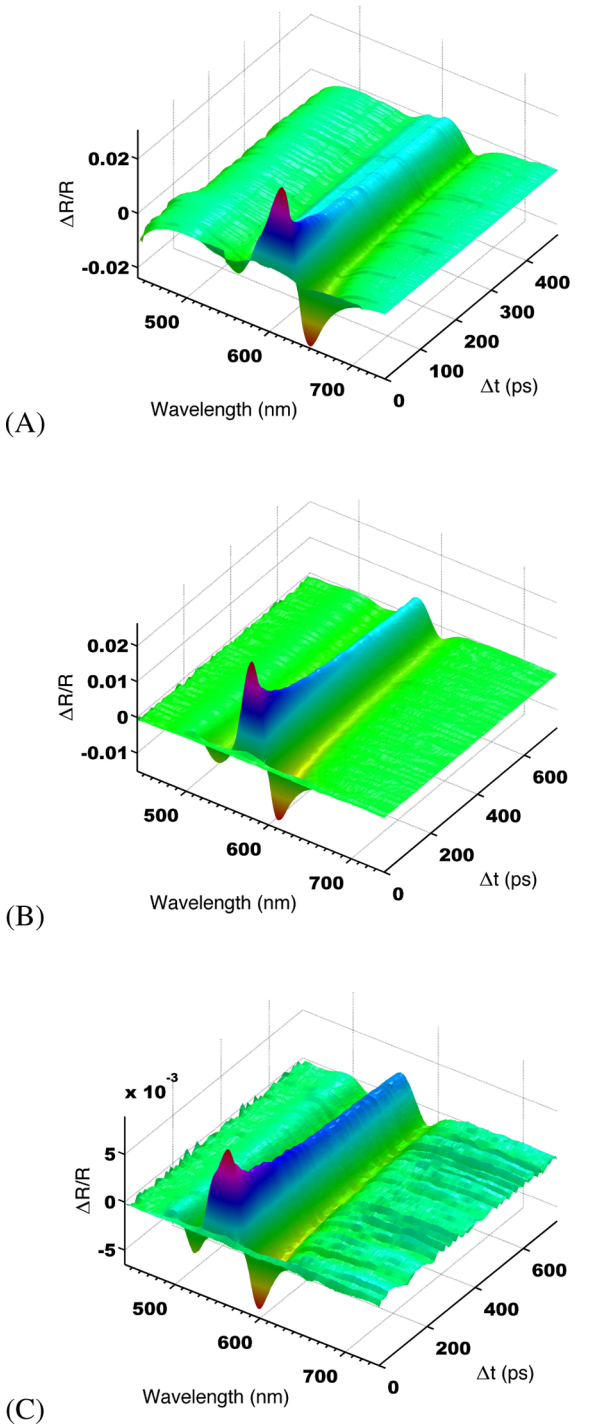

Figure 4. Transient reflectivity spectra of a Ag/CdSe nanocrystal film measured in the Kretschmann configuration with the probe pulses incident at (A) 45°, (B) 55°, and (C) 65°, with respect to the base of the prism.

Table 1. Fits of the Data Shown in Figure 3C to Biexponential Functions $y(t) = A_1 \exp(-t/\tau_1) + (1 - A_1) \exp(-t/\tau_2)$[a]

AOI (deg)	λ (nm)	A_1	τ_1 (ps)	τ_2 (ps)	$\langle\tau\rangle$ (ps)
45	614	0.507 (0.004)	9.2 (0.2)	117 (2)	62 (2)
55	572	0.518 (0.004)	50.1 (0.9)	964 (19)	490 (13)
65	554	0.450 (0.005)	54.2 (1.3)	1162 (26)	664 (20)
bare film	583	0.538 (0.005)	71.7 (1.6)	1954 (53)	941 (36)

[a]AOI, angle of incidence; values in parentheses correspond to standard error; $\langle\tau\rangle$ is an average decay rate.

dx.doi.org/10.1021/jp306830s | J. Phys. Chem. B 2013, 117, 4340−4346

feature to the blue side of the spectrum [see also Figure 3A (bottom)]. Similar lineshapes have been found in transient absorption studies of strongly interacting *J*-aggregates and Au nanorods[33] and *J*-aggregates with plasmons in perforated metal films[34] and have been assigned to direct excitation of the hybrid SPP−exciton states in the system.

To interpret the spectral shape observed, we again use the single Lorentzian model introduced above. Calculated transient reflectivity spectra are presented in Figure 3B (bottom) (details in Supporting Information). The model predicts the appearance of three bands in the $\Delta R/R$ spectra, two of which are negative, thus displaying qualitative agreement with the experimental results. Since this model only accounts for bleaches in the lowest-energy exciton transition, the similarity of the calculated and the experimental spectra implies a minimal contribution from transient heating effects in the metal. Note that bleaching or saturation of the exciton transition is expected to decrease the magnitude of the resonance splitting observed in the energy vs angle diagram of Figure 1 since the magnitude of this splitting is proportional to the density of dipoles interacting with the SPPs.[16] This effect is implicitly included in the Lorentzian model and is the reason for the more complicated spectra for the CdSe NQDs on Ag compared to glass. The Lorentzian model predicts an increase in the magnitude of the $\Delta R/R$ bands in going from 45° to 55° as is observed experimentally but fails to predict the strong decrease that occurs at 65°. This discrepancy most likely arises from contributions from the higher-energy exciton transitions in the CdSe NQDs, which are neglected in our calculation of $\varepsilon(\omega)$.

These considerations yield the following interpretation of the transient absorption spectra: the frequencies of the $\Delta R/R$ features depend on the coupling between the SPPs of the metal film and the CdSe excitons (which is controlled by the angle in our experiments), whereas their magnitude depends on the exciton population (which changes with time).

Now, we turn our attention to the kinetic aspects of the data. To this end, we have plotted in Figure 3C, the amplitude-normalized transient decays of the most intense $\Delta R/R$ features observed in Figure 4. These decays are all highly nonexponential, and the general trend observed is an increase in the decay times with an increase in the angle of incidence. These trends are more evident in the time constants obtained from the fits of the data using a biexponential function (summarized in Table 1), which indicate that the average decay time for the 45° data is an order of magnitude faster than that at 65°. At first glance, this result is counterintuitive since the state monitored at 65° has a higher energy than that at 45° and therefore should show faster dynamics.

To understand these results, it is instructive to consider the steady-state data shown in Figure 1C and the diagram shown in Figure 3D. The coupling between excitons in the CdSe NQDs and SPPs in the Ag film leads to the formation of two hybrid states (upper and lower branches, *U* and *L* in the energy dispersion diagram). These hybrid states can be written as linear combinations of the zeroth-order uncoupled exciton and SPP states[49] (we adopt here the sign convention of ref 49):

$$|U(k)\rangle = c_2(k)|\text{exciton}\rangle + c_1(k)|\text{SPP}(k)\rangle$$
$$|L(k)\rangle = -c_1(k)|\text{exciton}\rangle + c_2(k)|\text{SPP}(k)\rangle \quad (1)$$

where the wavevector (k) dependence of the coefficients and SPP wave functions has been explicitly noted. The square value of the coefficients is a measure of the relative exciton/plasmon contribution to the superposition. The values of $|c_1|^2$ and $|c_2|^2$ derived from the fits to the steady-state reflectivity measurements are plotted in Figure 3D. At the point of the avoided crossing in Figure 1C, both the upper and lower mixed states have equal exciton and SPP contributions as shown in Figure 3D. Note that the lifetimes of the zeroth−order exciton and SPP states are different, with the SPP state expected to have a shorter lifetime due to nonradiative processes.[50] As shown in Figure 4, the kinetics measured in the transient reflectivity measurements changes with the angle of incidence of the probe laser. The fastest decays in the $\Delta R/R$ spectra are observed at 45°, which corresponds to a situation where the lower-energy hybrid state has a strong plasmonic character; see Figure 3D. In contrast, at 65°, where the lower hybrid state is predominantly excitonic, the decays are slower, with time-constants close to that observed for the CdSe film on glass.

The transient reflectivity results can be interpreted in the following way. Excitation of the CdSe NQDs by the pump creates electron−hole pairs that rapidly relax to the lowest-energy excited state of the system. For the CdSe NQDs on glass, this is the lowest exciton state of the NQDs, whereas for the CdSe NQDs on Ag, it is the lower hybrid state $|L(k)\rangle$. In principle, there are other decay channels to be considered, including decay into $|U(k)\rangle$.[51] However, experiments on strongly coupled systems in optical microcavities[52−54] suggest that most of these incoherent excitations decay to the $|L(k)\rangle$ states on the time scales of our experiments. Thus, shortly after excitation, the system is in a mixed state that corresponds to a (incoherent) sum over the different $|L(k)\rangle$ states excited during energy relaxation of the photoexcited electron−hole pairs in the CdSe film. The transient reflectivity measurements monitor the recovery of the ground state population of the CdSe NQDs, and the time scale for this process is controlled by the lifetime of the lowest-energy excited state ($|L(k)\rangle$).

The lifetimes of the $|L(k)\rangle$ state vary with wavevector because the character of the state changes. At angles less than 45°, where the $|L(k)\rangle$ state has predominant SPP character, the coupled system can rapidly relax either nonradiatively through the SPP component of the $|L(k)\rangle$ hybrid state or by radiative emission into the SPP modes.[55,56] The radiative pathway is analogous to the lifetime reduction of emitters in optical microcavities due to the Purcell effect.[57−59] In contrast, at higher angles, the $|L(k)\rangle$ state has predominant exciton character, and the relaxation is similar to the CdSe NQDs on glass (there are no added decay channels from interaction with the SPP states). Thus, as the angle of incidence of the probe is changed, different dynamics are observed because different hybrid $|L(k)\rangle$ states come into play. Note that it is the lifetime of the $|L(k)\rangle$ state that is important in determining the dynamics in the transient reflectivity measurements, even at angles larger than 45° where the main contribution to the transient reflectivity spectra is from the $|U(k)\rangle$ state, as the $|L(k)\rangle$ state lifetime controls the ground state recovery.

CONCLUSIONS

Overall, the dynamics measured for coupled CdSe/Ag films in transient reflectivity measurements conducted in the Kretschmann geometry have a complicated wavevector dependence. Our results show that the measured dynamics is controlled by the composition of the lower hybrid exciton/SPP state $|L(k)\rangle$. Specifically, fast dynamics are obtained when the $|L(k)\rangle$ state has a predominant SPP character, and slower dynamics are

obtained when $|L(k)\rangle$ is predominantly excitonic. The decrease in the $|L(k)\rangle$ state lifetime can arise from either radiative emission into the SPP modes or nonradiative processes involving the SPP component of the wave function. In principle, these two pathways could be separated by time-resolved emission measurements, and we are currently attempting these experiments. These results are important for applications such as amplification of SPPs by optical pumping of a surrounding gain medium, in particular for the demonstration of this process in the strong coupling regime, where a prerequisite is the efficient population of the lower hybrid state branch.[53]

■ ASSOCIATED CONTENT

Supporting Information

AFM topography scans of the thin films. Detailed information on the Fresnel equation model of the reflectivity of the thin films and the biexponential fits to the kinetic data. This material is available free of charge via the Internet at http://pubs.acs.org.

■ AUTHOR INFORMATION

Corresponding Author

*E-mail: dgomez@unimelb.edu.au (D.E.G.); ghartlan@nd.edu (G.V.H.).

Notes

The authors declare no competing financial interest.

■ ACKNOWLEDGMENTS

D.E.G. would like to thank the Australian Academy of Science for support through its International Science Linkages program, the ARC for support through a Discovery Project DP110101767, and the Melbourne Materials Institute. S.S.L and G.V.H acknowledge support from the University of Notre Dame Strategic Research Initiative. We thank Prashant Kamat for use of his ultrafast laser system for the transient absorption experiments

■ REFERENCES

(1) Maier, S. *Plasmonics: Fundamentals and Applications*; Springer: New York, 2007.
(2) Lei, D. Y.; Appavoo, K.; Sonnefraud, Y.; Haglund, R. F., Jr.; Maier, S. A. *Opt. Lett.* **2010**, *35*, 3988−3990.
(3) Huang, F.; Baumberg, J. J. *Nano Lett.* **2010**, *10*, 1787−1792.
(4) Kossyrev, P.; Yin, A.; Cloutier, S.; Cardimona, D.; Huang, D.; Alsing, P.; Xu, J. *Nano Lett.* **2005**, *5*, 1978−1981.
(5) Dicken, M. J.; Sweatlock, L. A.; Pacifici, D.; Lezec, H. J.; Bhattacharya, K.; Atwater, H. A. *Nano Lett.* **2008**, *8*, 4048−4052.
(6) Dionne, J. A.; Diest, K.; Sweatlock, L. A.; Atwater, H. A. *Nano Lett* **2009**, *9*, 897−902.
(7) Gjonaj, B.; Aulbach, J.; Johnson, P. M.; Mosk, A. P.; Kuipers, L.; Lagendijk, A. *Nat. Photonics* **2011**, *5*, 360−363.
(8) Zheng, Y. B.; Yang, Y.-W.; Jensen, L.; Fang, L.; Juluri, B. K.; Flood, A. H.; Weiss, P. S.; Stoddart, J. F.; Huang, T. J. *Nano Lett.* **2009**, *9*, 819−825.
(9) Berrier, A.; Cools, R.; Arnold, C.; Offermans, P.; Crego-Calama, M.; Brongersma, S. H.; Gómez-Rivas, J. *ACS Nano* **2011**, *5*, 6226−6232.
(10) Liu, N.; Tang, M. L.; Hentschel, M.; Giessen, H.; Alivisatos, A. P. *Nat. Mater.* **2011**, *10*, 631−636.
(11) Schwartz, T.; Hutchison, J. A.; Genet, C.; Ebbesen, T. W. *Phys. Rev. Lett.* **2011**, *106*, 196405−1−196405−4.
(12) Wurtz, G. A.; Pollard, R.; Zayats, A. V. *Phys. Rev. Lett.* **2006**, *97*, 057402.
(13) Dintinger, J.; Robel, I.; Kamat, P.; Genet, C.; Ebbesen, T. *Adv. Mater.* **2006**, *18*, 1645−1648.
(14) Dintinger, J.; Klein, S.; Ebbesen, T. *Adv. Mater.* **2006**, *18*, 1267−1270.
(15) Wiederrecht, G. P.; Hall, J. E.; Bouhelier, A. *Phys. Rev. Lett.* **2007**, *98*, 083001.
(16) Vasa, P.; Pomraenke, R.; Cirmi, G.; De Re, E.; Wang, W.; Schwieger, S.; Leipold, D.; Runge, E.; Cerullo, G.; Lienau, C. *ACS Nano* **2010**, *4*, 7559−7565.
(17) Abb, M.; Albella, P.; Aizpurua, J.; Muskens, O. L. *Nano Lett.* **2011**, *11*, 2457−2463.
(18) MacDonald, K.; Zheludev, N. *Laser Photonics Rev.* **2010**, *4*, 562−567.
(19) Klimov, V. I., Ed. *Semiconductor and Metal Nanocrystals*; Marcel Dekker: New York, 2004.
(20) Canneson, D.; Mallek-Zouari, I.; Buil, S.; Quélin, X.; Javaux, C.; Mahler, B.; Dubertret, B.; Hermier, J.-P. *Phys. Rev. B* **2011**, *84*, 245423.
(21) Naiki, H.; Masuo, S.; Machida, S.; Itaya, A. *J. Phys. Chem. C* **2011**, *115*, 23299−23304.
(22) Song, J.-H.; Atay, T.; Shi, S.; Urabe, H.; Nurmikko, A. *Nano Lett.* **2005**, *5*, 1557−1561.
(23) Chen, Y.; Munechika, K.; Plante, I. J.-L.; Munro, A. M.; Skrabalak, S. E.; Xia, Y.; Ginger, D. S. *Appl. Phys. Lett.* **2008**, *93*, 053106.
(24) Komarala, V. K.; Bradley, A. L.; Rakovich, Y. P.; Byrne, S. J.; Gun'ko, Y. K.; Rogach, A. L. *Appl. Phys. Lett.* **2008**, *93*, 123102.
(25) Akimov, A. V.; Mukherjee, A.; Yu, C. L.; Chang, D. E.; Zibrov, A. S.; Hemmer, P. R.; Park, H.; Lukin, M. D. *Nature* **2007**, *450*, 402−406.
(26) Pacifici, D.; Lezec, H. J.; Atwater, H. A. *Nat. Photonics* **2007**, *1*, 402−406.
(27) Bellessa, J.; Bonnand, C.; Plenet, J. C.; Mugnier, J. *Phys. Rev. Lett.* **2004**, *93*, 036404.
(28) Bonnand, C.; Bellessa, J.; Plenet, J. C. *Phys. Rev. B* **2006**, *73*, 245330.
(29) Bonnand, C.; Bellessa, J.; Symonds, C.; Plenet, J. C. *Appl. Phys. Lett.* **2006**, *89*, 231119.
(30) Dintinger, J.; Klein, S.; Bustos, F.; Barnes, W. L.; Ebbesen, T. W. *Phys. Rev. B* **2005**, *71*, 035424.
(31) Sugawara, Y.; Kelf, T. A.; Baumberg, J. J.; Abdelsalam, M. E.; Bartlett, P. N. *Phys. Rev. Lett.* **2006**, *97*, 266808.
(32) Symonds, C.; Bonnand, C.; Plenet, J. C.; Brehier, A.; Parashkov, R.; Lauret, J. S.; Deleporte, E.; Bellessa, J. *New J. Phys.* **2008**, *10*, 065017.
(33) Hao, Y.-W.; Wang, H.-Y.; Jiang, Y.; Chen, Q.-D.; Ueno, K.; Wang, W.-Q.; Misawa, H.; Sun, H.-B. *Angew. Chem., Int. Ed.* **2011**, *50*, 7824−8.
(34) Salomon, A.; Genet, C.; Ebbesen, T. *Angew. Chem., Int. Ed.* **2009**, *48*, 8748−8751.
(35) Hakala, T. K.; Toppari, J. J.; Kuzyk, A.; Pettersson, M.; Tikkanen, H.; Kunttu, H.; Törmä, P. *Phys. Rev. Lett.* **2009**, *103*, 053602.
(36) Gómez, D. E.; Vernon, K. C.; Mulvaney, P.; Davis, T. J. *Appl. Phys. Lett.* **2010**, *96*, 073108.
(37) Gómez, D. E.; Vernon, K. C.; Mulvaney, P.; Davis, T. J. *Nano Lett.* **2010**, *10*, 274−278.
(38) Giebink, N. C.; Wiederrecht, G. P.; Wasielewski, M. R. *Appl. Phys. Lett.* **2011**, *98*, 081103.
(39) van Embden, J.; Mulvaney, P. *Langmuir* **2005**, *21*, 10226−10233.
(40) Jasieniak, J.; Smith, L.; van Embden, J.; Mulvaney, P.; Califano, M. *J. Phys. Chem. C* **2009**, *113*, 19468−19474.
(41) Raether, H. In *Physics of Thin Films*; Hass, G., Francombe, M. H., Hoffman, R. W., Eds.; Academic Press: New York, 1977; Vol. *9*, Chapter 3, pp 145−262.
(42) Tvrdy, K.; Kamat, P. V. *J. Phys. Chem. A* **2009**, *113*, 3765−3772.
(43) Klimov, V. I. *J. Phys. Chem. B* **2000**, *104*, 6112−6123.
(44) Khitrova, G.; Gibbs, H. M.; Jahnke, F.; Kira, M.; Koch, S. W. *Rev. Mod. Phys.* **1999**, *71*, 1591−1639.
(45) Klimov, V. *J. Phys. Chem. B* **2000**, *104*, 6112−6123.

(46) Norris, D. J.; Sacra, A.; Murray, C. B.; Bawendi, M. G. *Phys. Rev. Lett.* **1994**, *72*, 2612−2615.
(47) Klimov, V. I.; McBranch, D. W.; Leatherdale, C. A.; Bawendi, M. G. *Phys. Rev. B* **1999**, *60*, 13740−13749.
(48) Klimov, V.; Hunsche, S.; Kurz, H. *Phys. Rev. B* **1994**, *50*, 8110−8113.
(49) Cohen-Tannoudji, C.; Diu, B.; Laloë, F. *Quantum Mechanics*; John Wiley and Sons: New York, 1977; Vol. *1*.
(50) Lamprecht, B.; Krenn, J. R.; Schider, G.; Ditlbacher, H.; Salerno, M.; Felidj, N.; Leitner, A.; Aussenegg, F. R.; Weeber, J. C. *Appl. Phys. Lett.* **2001**, *79*, 51−53.
(51) Agranovich, V. M.; Gartstein, Y. N.; Litinskaya, M. *Chem. Rev.* **2011**, *111*, 5179−5214.
(52) Virgili, T.; Coles, D.; Adawi, A. M.; Clark, C.; Michetti, P.; Rajendran, S. K.; Brida, D.; Polli, D.; Cerullo, G.; Lidzey, D. G. *Phys. Rev. B* **2011**, *83*, 245309.
(53) Kena-Cohen, S.; Forrest, S. R. *Nat. Photonics* **2010**, *4*, 371−375.
(54) Coles, D. M.; Michetti, P.; Clark, C.; Tsoi, W. C.; Adawi, A. M.; Kim, J.-S.; Lidzey, D. G. *Adv. Funct. Mater.* **2011**, *21*, 3691−3696.
(55) Okamoto, K.; Niki, I.; Scherer, A.; Narukawa, Y.; Mukai, T.; Kawakami, Y. *Appl. Phys. Lett.* **2005**, *87*, 071102.
(56) Neogi, A.; Lee, C.-W.; Everitt, H. O.; Kuroda, T.; Tackeuchi, A.; Yablonovitch, E. *Phys. Rev. B* **2002**, *66*, 153305.
(57) Kress, A.; Hofbauer, F.; Reinelt, N.; Kaniber, M.; Krenner, H. J.; Meyer, R.; Böhm, G.; Finley, J. J. *Phys. Rev. B* **2005**, *71*, 241304.
(58) Gerard, J.-M.; Gayral, B. *J. Lightwave Technol.* **1999**, *17*, 2089−2095.
(59) Vahala, K. J. *Nature* **2003**, *424*, 839−846.